A MAXIMUM PRINCIPLE FOR BELTRAMI COLOR FLOW

LORINA DASCAL* AND NIR A. SOCHEN†

Abstract. We study, in this work, the maximum principle for the Beltrami color flow and the stability of the flow's numerical approximation by finite difference schemes. We discuss, in the continuous case, the theoretical properties of this system and prove the maximum principle in the strong and the weak formulations. In the discrete case, all the second order explicit schemes, that are currently used, violate, in general, the maximum principle. For these schemes we give a theoretical stability proof, accompanied by several numerical examples.

Keywords: Maximum Principle, Beltrami Framework, Parabolic PDE's, Finite difference schemes.

1. Introduction. The maximum principle in its various forms is a powerful and instrumental tool for establishing results concerning existence, uniqueness and other qualitative properties of linear and nonlinear partial differential equations. A complete overview of this subject until 1967 can be found in [16].

We are interested in the property of maximum principle for Beltrami color flow in the context of Scale-Space theory. This theory claims that significant information exists in all levels of resolution/scale of the image. It is important to create a simplification process, called a "Scale-Space", from which the information can be extracted.

The notion of causality, in the context of image processing and especially in scale-space and de-noising was put forward in the work of Koenderink [12] . In the one-dimensional case it is desirable that the simplification process of the signal will not create new maxima. This demand, together with homogeneity, lead to filtering with a Gaussian kernel. The convolution of this kernel with the initial image is the solution of the linear diffusion equation with the initial image as initial condition. For higher dimensional signals the non-creation of new maxima can not be achieved. It is usually replaced by a new principle – the non creation of new level sets. This new principle is called, in the scale-space literature "the causality principle". It is directly related, in the scalar case, to the extremum principle as observed by Hummel [8]. The extremum principle is taken as the natural generalization of the causality principle to the vectorial case.

Moreover, the relevance of investigating the maximum principle for the Beltrami flow and other PDEs based models can be seen through the work of Alvarez et al. [1]. In this paper, the authors propose a rigorous connection between scale space analysis and PDEs. They start from a very natural set of filtering axioms and show that the resulting filtered image must necessarily be the solution of a second order, fully nonlinear parabolic PDE. The maximum principle is one of their axioms, which is imposed so that smoothing of the original image is made with no enhancement.

The problem of the discrete maximum principle was studied in many works. This issue is important as it ensures that intensity values in the evolving image are constrained by the initial image values and do not grow without bounds. Perona and Malik [14] proposed a numerical scheme which satisfies this property as proved in

*Department of Applied Mathematics, Tel Aviv University, Ramat-Aviv, Tel-Aviv 69978, Israel, (lorina@math.tau.ac.il).

†Department of Applied Mathematics, Tel Aviv University, Ramat-Aviv, Tel-Aviv 69978, Israel, (sochen@math.tau.ac.il).

[24]. Also the PDE introduced by Catte et al. [3] was proven to satisfy the discrete maximum principle [24].

In this paper we treat the Beltrami flow for color images and study two aspects of the maximum principle (continuous and discrete). First we deal with the continuous formulation of the maximum principle and prove it for both the strong and the weak formulations. The motivation for considering these two formulations is threefold: First, the strong formulation is presented here in order to check the validity of the maximum principle for a smooth solution. Second, this property is generalized for a class of non-regular functions via a weak formulation of the maximum principle. In what concerns the weak formulation, we follow Florack's [6], and later Mumford and Gidas' [13] duality approach. In these works the image is conceived as a generalized function. The duality approach describes the sensor space (also called "device space") as a functional space. The data we usually process, which result from the interaction of the physical/optical data and the sensor, are modelled as an inner product of the sensor function and the "true image". In this context, the set of images is equivalent to the set of linear functionals on the sensor functional space. It is natural from this point of view to study the flow equations on the image space directly. We are able to do so by defining generalized (weak) solutions to our flow equations. The third reason lies in the fact that to achieve a proper analysis of images, we must consider functions with less regular structure than the smooth functions we dealt with in the strong formulation. This again leads to the study of weak solutions.

To the best of our knowledge, for highly nonlinear and strongly coupled systems as the one we describe here, no mathematical analysis has been performed even for smooth functions. In previous works [4], [2] well-posedness and the maximum principle were treated for scalar valued functions only and for initial data of Lipschitz type, which excludes discontinuous functions.

In the last part of the paper we study the discrete maximum principle for a certain explicit difference scheme by which the nonlinear differential equation is approximated. We show that to approximate the various derivatives to a given order is not enough to guarantee the maximum principle. This scheme can *violate* the maximum principle. We present, though, a proof of the stability of this scheme along with examples that clearly demonstrate stability, while failing to obey the maximum principle.

The paper is organized as follows: In section 2 we review the Beltrami framework. In section 3 we deal with the continuous formulation of the maximum principle. We prove the extremum principle for the strong solution of the parabolic quasi-linear system that characterizes the Beltrami color flow. In section 4 we introduce a weak (generalized) solution for this system and prove the extremum principle in a weak formulation. In section 5 we discuss the properties of the second-order central difference scheme, which in general violates the maximum principle. For this scheme we give a theoretical stability proof. In section 6 we present numerical results. We summarize and conclude in section 7.

2. The Beltrami Framework. Let us briefly review the Beltrami framework for non-linear diffusion in computer vision [9, 20, 21].

The space of interest in computer vision such as images, texture, disparity in stereo-vision, optical flow, distortion in registration and more, is represented as a *fiber bundle*. The base manifold is the image domain. We consider in this work a flat and compact domain. A non-flat domain is treated, for example, in [19]. The feature space, be it gray-values, color, optical flow, texture, etc, is the fiber space.

Any particular image, or vector field, is a *section* of this fiber bundle. We assume that the Riemannian structure can be defined for the base manifold and for the fiber bundle. Thus, we represent an image and other local features as an embedding map of a Riemannian manifold in a higher dimensional space-the fiber bundle. The simplest example is a gray-level image which is represented as a 2D surface embedded in $\mathbb{R}^3$. We denote the map by $X : \Sigma \to \mathbb{R}^3$, where Σ is a two-dimensional surface, and we denote the local coordinates on it by (σ^1, σ^2). The map U is given in general by $(U^1(\sigma^1, \sigma^2), U^2(\sigma^1, \sigma^2), U^3(\sigma^1, \sigma^2))$. In our example we represent map U as follows: $(U^1 = \sigma^1, U^2 = \sigma^2, U^3 = I(\sigma^1, \sigma^2))$. We choose on this surface a Riemannian structure, namely, a metric. The metric is a positive definite and a symmetric 2-tensor that may be defined through the local distance measurements:

$$ds^2 = g_{11}(d\sigma^1)^2 + 2g_{12}d\sigma^1 d\sigma^2 + g_{22}(d\sigma^2)^2.$$

The canonical choice of coordinates in image processing is Cartesian. For such choice, which we follow in the rest of the paper, we identify $\sigma^1 = x^1$ and $\sigma^2 = x^2$. We use below the Einstein summation convention in which a pair of upper and lower identical indices is summed over. With this convention, the above equation is written as $ds^2 = g_{ij}dx^i dx^j$. We denote the elements of the inverse of the metric by superscripts $g^{ij} = (g^{-1})_{ij}$, and the determinant by $g = \det(g_{ij})$.

Once the image is defined as an embedding mapping of Riemannian manifolds it is natural to look for a measure on this space of embedding maps.

2.1. Polyakov Action: A Measure on the Space of Embedding Maps. Denote by (Σ, g) the image manifold and its metric, and by (M, h) the space-feature manifold and its metric. Then the functional $S[U]$ attaches a real number to a map $U : \Sigma \to M$:

$$S[U^a, g_{ij}, h_{ab}] = \int dV ||dU||^2_{g,h},$$

where dV is a volume element that is expressed in a local coordinate system as $dV = \sqrt{g}dxdy$. The integrand $||dU||^2_{g,h}$ is the Riemannian Frobenius norm of the tangent map. It is expressed in a local coordinate system by $||dU||^2_{g,h} = (\partial_{x_i}U^a)g^{ij}(\partial_{x_j}U^b)h_{ab}$. This functional, for $m = 2$ and $h_{ab} = \delta_{ab}$, was first proposed by Polyakov [15] in the context of high energy physics, and the theory is known as the *string theory*.

Let us formulate the Polyakov action in matrix form: (Σ, G) is the image manifold and its metric as before. Similarly, (M, H) is the spatial-feature manifold and its metric. Define

$$A^{ab} = (\vec{\nabla}U^a)^t G^{-1}\vec{\nabla}U^b.$$

The map $U : \Sigma \to M$ has a weight

$$S[U, G, H] = \int d^m\sigma\sqrt{g}\ \mathrm{Tr}(AH),$$

where m is the dimension of Σ and $g = \det(G)$.

Using standard methods in the calculus of variations, the Euler-Lagrange equations with respect to the embedding (assuming Euclidean embedding space) are (see [20] for explicit derivation):

$$0 = -\frac{1}{2\sqrt{g}}h^{ab}\frac{\delta S}{\delta U^b} = \frac{1}{\sqrt{g}}\partial_{x_i}(\sqrt{g}g^{ij}\partial_{x_j}U^a), \tag{2.1}$$

or in matricial form

$$0 = -\frac{1}{2\sqrt{g}} h^{ab} \frac{\delta S}{\delta U^b} = \underbrace{\frac{1}{\sqrt{g}} \mathrm{div}\left(D \nabla U^a\right)}_{\Delta_g U^a}. \tag{2.2}$$

(where the matrix $D = (d^{ij})_{i,j=1,2} = \sqrt{g} G^{-1}$). The extension for non-Euclidean embedding space is treated in [10, 21, 22]. The elements of the induced metric for color images with Cartesian color coordinates are:

$$g_{ij} = \delta_{ij} + \beta^2 \sum_{a=1}^{3} U^a_{x_i} U^a_{x_j}, \tag{2.3}$$

where $\beta > 0$ is the ratio between the spatial and color distances, and the subscript of U denotes partial derivation. Note that this metric is different from the Di Zenzo matrix [26] (which is not a metric since it is not positive definite). A generalization of Di Zenzo's gradient for color images was investigated in [25] by constructing an anisotropic vector-valued diffusion model with a common tensor-valued structure descriptor.

The value of the parameter β, present in the elements of the metric g_{ij}, is very important and determines the nature of the flow. In the limit $\beta \to 0$, for example, the flow degenerates to the decoupled channel by channel linear diffusion flow. In the other limit $\beta \to \infty$ we get a new nonlinear flow. The gray-value analogue of this limit is the Total Variation flow of [17] (see details in [21]).

Since (g_{ij}) is positive definite, $g \equiv \det(g_{ij}) > 0$ for all σ^i. This factor is the simplest one that does not change the minimization solution while giving a reparameterization invariant expression. The operator that acts on U^a is the natural generalization of the Laplacian from flat spaces to manifolds and is called the Laplace-Beltrami operator, denoted by Δ_g.

The non-linear diffusion or scale-space equation emerges via the gradient descent minimization:

$$U^a_t = \frac{\partial}{\partial t} U^a = -\frac{1}{2\sqrt{g}} h^{ab} \frac{\delta S}{\delta U^b} = \Delta_g U^a. \tag{2.4}$$

The mathematical properties of this system, together with the initial and boundary conditions which will be detailed below, are studied in the rest of the paper with an emphasis on the extremum principle.

3. The Extremum Principle in the Strong Formulation. Here we establish the maximum principle for the strong solution of the initial boundary-value problem which characterizes the Beltrami color flow. We refer to the term 'strong solutions' when we talk about solutions which are functions with some smoothness criteria that we detail below. Let us first introduce some notations: We denote the image domain by Ω. It is a bounded open domain in $\mathbb{R}^2$. We denote by $\partial\Omega$ the boundary of Ω. We define the space-time cylinder $Q_T = \Omega \times (0, T)$, and denote its lateral surface by $S_T = \{(x, t) | x \in \partial\Omega, t \in (0, T)\}$. We also define the parabolic boundary by the union of the bottom and the lateral boundaries of the cylinder $\Gamma_T = \Omega \bigcup S_T$.

The PDE is the gradient descent equation for the Polyakov action as was described in the previous section. We rearrange the equation by explicitly carrying out the calculation of the derivation operator *div*. The result is the sum of two terms: The

first term results from applying the *div* to $\sqrt{g}G^{-1}$, and the second from applying the *div* to the gradient's components $U^a_{x_i}$. Remember that the metric, and consequently its inverse and its determinant, depends on first order derivatives. Applying the *div* operator to it gives rise to second order derivatives of the different channels as well. Rearranging the right hand side of Eq. (2.4) according to the second order derivatives, and the coefficients thereof, we arrive at the following coupled system of PDEs:

$$U^a_t = (F^a_{\ b})^{ij} U^b_{x_i x_j}, \quad (x,t) \in Q_T \ , \tag{3.1}$$

where $a, b = 1, 2, 3$ are indices in color space, $i, j = 1, 2$ are spatial indices and summation is applied to all repeated indices. Note that $(F^a_{\ b})$ are nine 2x2 matrices. Denote by $H^a = (U^a_{x_i x_j})_{ij=1}^2$ the Hessian of U^a. This system of PDEs can be written in terms of a trace in the spatial domain as

$$U^a_t = \text{Trace}\left(F^a_{\ b} H^b\right) \ , \quad (x,t) \in Q_T \ , \tag{3.2}$$

where, as before, the repeated b index implies a summation over the color indices.

The system of PDEs for which we establish the extremum principle is

$$U^a_t = \Delta_g U^a = \frac{1}{\sqrt{g}} \text{div}(D \nabla U^a), \quad U^a = R, G, B, \tag{3.3}$$

where D is defined as before: $D = \sqrt{g}G^{-1}$.

The initial and boundary conditions are

$$U^a(x,0) = U^a_0(x), \quad x \in \Omega \tag{3.4}$$

$$D\vec{\nabla} U^a \cdot \vec{n}\Big|_{S_T} = 0, \tag{3.5}$$

where $\vec{n}$ is the outer normal to $\partial\Omega$ and the dot product denotes, as usual, the Euclidean scalar product on $\mathbb{R}^2$.

LEMMA 3.1. *The nine 2x2 matrices $(F^a_{\ b})$ are symmetric, positive definite, and their elements $(F^a_{\ b})^{ij}$ are rational functions of the first derivatives of the different channels. These matrix elements are, moreover,* uniformly bounded functions *on Q_T.*

Proof. The proof is by direct calculation. One finds for example:

$$\begin{aligned}
\left(F^2_{\ 1}\right)^{11} &= -R_x G_x \frac{g_{22}^2}{g^2} + (R_x G_y + R_y G_x)\frac{g_{12} g_{22}}{g^2} - \frac{R_y G_y}{g}\left(1 + \frac{g_{12}^2}{g}\right) \\
\left(F^2_{\ 1}\right)^{12} &= \left(F^2_{\ 1}\right)^{21} = \frac{R_x G_y + R_y G_x}{g} - \frac{R_x G_y + R_y G_x}{g^2} g_{11} g_{22} - \\
&\qquad \frac{R_x G_y + R_y G_x}{g^2} g_{12}^2 + 2\frac{R_x G_x g_{22} + R_y G_y g_{11}}{g^2} g_{12}^2 \\
\left(F^2_{\ 3}\right)^{22} &= -R_y G_y \frac{g_{11}^2}{g^2} + (R_x G_y + R_y G_x)\frac{g_{11} g_{12}}{g^2} - \frac{R_x G_x}{g}(1 + \frac{g_{12}^2}{g})
\end{aligned} \tag{3.6}$$

(here we denoted by R, G, B the three components of the color vector $\overrightarrow{U}$).

These are rational functions of the first derivatives. The diagonal elements of $(F^a_{\ b})$ are strictly positive (by a direct check), and the negativity of the discriminant implies the positive definiteness of these matrices. One can verify directly that the coefficients are bounded functions of the first derivatives. These properties are verified, along the same lines for all matrices. □

Next we state the maximum principle for the strong solutions of the coupled system of PDEs (3.3), with initial data (3.4) and boundary condition (3.5).

THEOREM 3.2. *Let $\overrightarrow{U_0} \in C^2(\Omega)$. Then a solution $\overrightarrow{U} \in C^{2,1}(\bar{Q}_T)$ satisfies the following maximum principle:*

$$\begin{aligned} &1) \quad \max_{\bar{Q}_T} \sum_{a=1}^{3} U^a = \max_{\Omega} \sum_{a=1}^{3} U_0^a \\ &2) \quad \max_{\bar{Q}_T} U^a = \max_{\Omega} U_0^a. \end{aligned} \tag{3.7}$$

Proof.

Note that assertion 2 does not imply, in principle, assertion 1. We start by proving assertion 1. Consider the following system of inequalities

$$V_t^a < (F^a_{\ b})^{ij} V^b_{x_i x_j}, \quad (x,t) \in Q_T \ , \tag{3.8}$$

where $F^a_{\ b} = F^a_{\ b}(\nabla \vec{V})$.

We now show that a smooth solution of this system of inequalities satisfies

$$\max_{\bar{Q}_T} \sum_{a=1}^{3} V^a = \max_{\Gamma_T} \sum_{a=1}^{3} V^a. \tag{3.9}$$

Let $\bar{V} = \sum_{a=1}^{3} V^a$ and suppose on the contrary that the maximum of $\bar{V}$ is attained at an interior point $(x_0, t_0) \in \bar{Q}_T - \Gamma_T$. This assumption leads to a contradiction as follows: The maximality at the point (x_0, t_0) implies:

$$\bar{V}_t|_{(x_0,t_0)} \geq 0 \quad (\bar{V}_t|_{(x_0,t_0)} = 0 \quad \text{if} \quad 0 \leq t_0 < T). \tag{3.10}$$

Based on (2.1), the system of inequalities (3.8) is equivalent to

$$V_t^a < \frac{1}{\sqrt{g}} \partial_{x_i} (g^{ij} \sqrt{g} \partial_{x_j} V^a), \quad (x,t) \in Q_T. \tag{3.11}$$

Since the Laplace-Beltrami operator that acts on the components depends only on the geometry, the sum of components obeys the same inequality:

$$\bar{V}_t < \frac{1}{\sqrt{g}} \partial_{x_i} (g^{ij} \sqrt{g} \partial_{x_j} \bar{V}). \tag{3.12}$$

On the other hand carrying out the *div* computation explicitly we rewrite this inequality as

$$\frac{1}{\sqrt{g}} \partial_{x_i} (g^{ij} \sqrt{g} \partial_{x_j} \bar{V}) = g^{ij} \bar{V}_{x_i x_j} + \omega^j \bar{V}_{x_j}.$$

The functions ω^j depend on the first and second derivatives of each of the components of the color vector. They are bounded on Q_T by the smoothness of $\overrightarrow{V} \in C^{2,1}(\bar{Q}_T)$.

The positive definiteness of the matrix g^{ij} and the maximality at the point (x_0, t_0) imply

$$\frac{1}{\sqrt{g}} \partial_{x_i} (g^{ij} \sqrt{g} \partial_{x_j} \bar{V})|_{(x_0,t_0)} = g^{ij} \bar{V}_{x_i x_j}|_{(x_0,t_0)} < 0. \tag{3.13}$$

Clearly (3.10) and (3.13) contradict (3.12). We conclude that (3.9) holds for a solution of the system of inequalities (3.8).

Using the result for the solution of the system of inequalities, we prove the result concerning the solution $\vec{U}$ of our system (3.3). We define $W^a = U^a - \epsilon t$ and $\bar{W} = \sum_1^3 W^a$, $\bar{U} = \sum_1^3 U^a$. Then $\nabla W^a = \nabla U^a$, $g_{ij}(\vec{W}) = g_{ij}(\vec{U})$ and we obtain the following inequalities:

$$W_t^a - \frac{1}{\sqrt{g}}\partial_{x_i}(g^{ij}\sqrt{g}\partial_{x_j}W^a) = U_t^a - \frac{1}{\sqrt{g}}\partial_{x_i}(g^{ij}\sqrt{g}\partial_{x_j}U^a) - 3\epsilon < 0, \tag{3.14}$$

Since $\vec{W} = (W^a)_{a=1,2,3}$ satisfies (3.14), it follows that

$$\max_{\bar{Q}_T}\bar{W} = \max_{\Gamma_T}\bar{W}.$$

Letting $\epsilon \to 0$ we establish that

$$\max_{\bar{Q}_T}\bar{U} = \max_{\Gamma_T}\bar{U}.$$

Due to the boundary condition (3.5), the maximum cannot be attained on S_T (see [16]). Therefore assertion 1 is proved.

Next we prove assertion 2. Observe first that the off-diagonal matrices F_b^a with $a \neq b$ can be written as $U_{x_i}^a$ times a bounded function. Taking, for example, $(a, b) = (1, 2)$, one finds by rearranging the terms in (3.1) that

$$(F_2^1)^{ij} = U_{x_1}^1 \cdot f_1^{ij}(\nabla\overrightarrow{U}) + U_{x_2}^1 \cdot f_2^{ij}(\nabla\overrightarrow{U}); \tag{3.15}$$

So if $i = 1, j = 1$, for example, then

$$f_1^{11} = -U_{x_1}^2\frac{g_{22}^2}{g^2} + U_{x_2}^2\frac{g_{12}g_{22}}{g^2}, \quad f_2^{11} = U_{x_1}^2\frac{g_{12}g_{22}}{g^2} + U_{x_2}^2(\frac{g_{22}^2}{g^2} + \frac{1}{g}).$$

One can write the other off-diagonal matrices similarly. For the structure of the induced metric, we can easily see that:

$$g \geq 1, \quad \frac{g_{ij}}{g} \leq 1, \quad \text{for all} \quad i, j = 1, 2. \tag{3.16}$$

Since the solution $\overrightarrow{U}$ is in $C^{2,1}(\bar{Q}_T)$ one can readily establish, using (3.16), that the functions f_1^{ij}, f_2^{ij} are bounded on Q_T. We can, therefore, write the first equation of the system (3.1),(3.4),(3.5) in the following form:

$$U_t^1 = (F_1^1)^{ij}U_{x_ix_j}^1 + U_{x_ix_j}^2(U_{x_1}^1 f_1^{ij} + U_{x_2}^1 f_2^{ij}) + U_{x_ix_j}^3(U_{x_1}^1 g_1^{ij} + U_{x_2}^1 g_2^{ij}), \tag{3.17}$$

where g_1^{ij}, g_2^{ij} are, as above, bounded functions depending on the first derivatives of the vector solution $\overrightarrow{U}$. We rewrite this equation:

$$U_t^1 = (F_1^1)^{ij}U_{x_ix_j}^1 + T^iU_{x_i}^1,$$

where T^i are continuous functions on a compact domain and therefore bounded functions. Again using the maximality of the point (x_0, t_0), the positive definiteness of the matrix F_1^1 and similar reasoning to the proof of assertion 1, we can conclude that

$$\max_{\bar{Q}_T} U^1 = \max_{\Omega} U_0^1.$$

For the other two components the proof is the same, mutatis mutandis. Thus assertion 2 is proven. □

In the next section we define a weak solution for the Beltrami color flow and prove that it obeys the extremum principle if it exists.

4. Weak Formulation of the Extremum Principle. In this section we define a weak solution of the system (3.3), (3.4),(3.5) under the smoothness assumptions that are detailed below. We further prove the extremum principle for this type of solution.

Let us introduce the following notations:

Denote by $V(Q_T)$ the space of functions which belong to $L^2(Q_T)$ and have first weak derivatives satisfying: $\nabla u \in L^\infty(Q_T)$, $u_t \in L^\infty(Q_T)$.

The Sobolev space $W_r^{p,q}$ is the space of functions, for which the L_r norm of their first generalized p spatial derivatives and q time derivatives, is finite (below we omit the second superscript for functions on the spatial domain only).

First we define a weak solution as follows:

DEFINITION 4.1. *A weak solution of the system (3.3), with initial and boundary conditions (3.4),(3.5), is a vector function $\vec{U} \in V(Q_T)$ such that for any vector function $\vec{\eta} \in V(Q_T)$ (i.e. each of the components of the vector are in $V(Q_T)$), the following integral identities hold for almost all $t \in [0,T]$:*

$$\int_{Q_T} U_t^a \eta^a \sqrt{g}\, dxdt + \int_{Q_T} g^{ij} U_{x_i}^a \eta_{x_j}^a \sqrt{g}\, dxdt = 0. \tag{4.1}$$

REMARK 4.1. *The integral $\int_\Omega \sqrt{g}\, dx$ means the area of the two dimensional manifold embedded in R^5.*

REMARK 4.2. *Florack [6], in viewing an image as a tempered distribution (see [18]), adopted the space of the so called "slow growth" functions (smooth functions of rapid decay) as the sensor space. In this paper we take $V(Q_T)$ as the sensor functional space, which we choose in accordance with the weak formulation of our problem.*

Next we prove that if a weak solution exists and it satisfies $\nabla(\vec{U_t}) \in L^\infty(Q_T)$, the following weak extremum principle holds:

THEOREM 4.1. *Assume the initial data $\vec{U_0} \in W_2^1(\Omega)$.*

For a weak solution of the system (3.3),(3.4),(3.4) such that $\nabla(\vec{U_t}) \in L^\infty(Q_T)$ we have for almost all $(x,t) \in Q_T$:

$$ess\inf_{\Omega} U_0^a(x) \le U^a(x,t) \le ess\sup_{\Omega} U_0^a(x). \tag{4.2}$$

Proof. We prove (4.2) for one of the components.

We divide the cylinder Q_T into a finite number of cylinders of equal height $Q_{t_s} = \Omega \times (t_{s-1}, t_s)$ where $t_s = \dfrac{Ts}{N}$ and $s = 1, 2, ...N$.

For the cylinder Q_{t_1} we denote

$k_a = \operatorname{ess\,sup}_{\Omega} U_0^a(x)$ and $(U^a)^{k_a} = \max\{0, U^a - k_a\}$ for $(x,t) \in \Omega \times (0, t_1)$.

Choose the test function $\eta^1 = R^{k_1}$. Note that by the hypothesis, $\vec{U} \in V(Q_T)$, and therefore the choice of such η is justified. Identity (4.1) for component R is now:

$$\int_{Q_{t_1}} R_t R^{k_1}\sqrt{g}dxdt + \int_{Q_{t_1}} d^{ij} R_{x_i} R^{k_1}_{x_j}\, dx\, dt = 0. \tag{4.3}$$

Since the matrix D ($D = \sqrt{g}G^{-1}$) depends on the gradient $\nabla\vec{U}$ and $\nabla\vec{U} \in L^\infty(Q_{t_1})$, we have that D is a uniformly positive definite matrix, so there exists a constant $\nu > 0$ such that

$$d^{ij}(\nabla\bar{U})R_{x_i}R^{k_1}_{x_j} \geq \nu|\nabla R^{k_1}|^2 \quad \text{a.e.} \quad (x,t) \in Q_{t_1}.$$

Therefore, (4.3) for the component R becomes:

$$\int_{Q_{t_1}} R_t R^{k_1}\sqrt{g}dxdt + \nu\int_{Q_{t_1}} |\nabla R|^2\, dx\, dt \leq 0. \tag{4.4}$$

Since for almost all $t \in (0, t_1)$:

$$\int_\Omega R_t(x,t)R^{k_1}(x,t)\, dx = \frac{1}{2}\frac{d}{dt}\int_\Omega \Big(R^{k_1}(x,t)\Big)^2\, dx,$$

we get

$$\begin{aligned}\int_{Q_{t_1}} R_t R^{k_1}\sqrt{g}\, dx\, dt &= \frac{1}{2}\int_{Q_{t_1}} ((R^{k_1})^2)_t\sqrt{g}\, dx\, dt \\ &= \frac{1}{2}\Big(\int_\Omega (R^{k_1})^2\sqrt{g}\Big|_0^{t_1} dx - \int_{Q_{t_1}} (R^{k_1})^2(\sqrt{g})_t\, dx\, dt\Big)\,, \end{aligned}\tag{4.5}$$

and using 4.4 we get

$$\begin{aligned}\frac{1}{2}\int_\Omega \Big(R^{k_1}(x,t)\Big)^2\Big|_{t=t_1} dx + \nu\int_{Q_{t_1}} |\nabla R^{k_1}|^2 dxdt \leq &\frac{1}{2}\int_{Q_{t_1}} (R^{k_1})^2(\sqrt{g})_t\, dx\, dt \\ &+\frac{1}{2}\int_{Q_{t_1}} (R^{k_1}_0)^2\sqrt{g_0}\, dx. \end{aligned}\tag{4.6}$$

Since $\vec{U_0} \in W_2^1(\Omega)$ and $R^{k_1}(x,0) = R^{k_1}_0 = 0$, then $\int_{Q_{t_1}} (R^{k_1}_0)^2\sqrt{g_0}\, dx = 0$ and (4.6) becomes:

$$\frac{1}{2}\max_{0\leq t\leq t_1}\int_\Omega \Big(R^{k_1}(x,t)\Big)^2 dx + \nu\int_{Q_{t_1}} |\nabla R^{k_1}|^2\, dx\, dt \leq \frac{1}{2}\int_{Q_{t_1}} (R^{k_1})^2(\sqrt{g})_t\, dx\, dt. \tag{4.7}$$

Denote by $||\cdot||_{V(Q_T)}$ the norm on the space $V(Q_T)$, where

$$||u||_{V(Q_T)} = \max_{0\leq t\leq T}||u||_{L^2(\Omega)} + \sqrt{\int_{Q_T} u_x^2(x,t)\, dx\, dt}.$$

By assumption $\vec{U}_{tx} \in L^\infty(Q_T)$ and then there exists a positive constant C such that $C = \sup_{Q_T}(\sqrt{g})_t$.

The Cauchy-Schwartz inequality leads us to:

$$\int_{Q_{t_1}} (R^{k_1})^2(\sqrt{g})_t \, dx\, dt \leq C \int_{Q_{t_1}} (R^{k_1})^2 \, dx\, dt$$
$$\leq Ct_1(\max_{0\leq t\leq t_1} ||R^{k_1}||_{L^2(\Omega)})^2 \leq Ct_1||R^{k_1}||^2_{V(Q_{t_1})} \qquad (4.8)$$

Therefore (4.7) becomes:

$$\min\{\frac{1}{2},\nu\}||R^{k_1}||^2_{V(Q_{t_1})} \leq \frac{C}{2}t_1 \quad ||R^{k_1}||^2_{V(Q_{t_1})}.$$

Then for sufficiently small t_1 such that

$$\frac{C}{2}t_1 < \min\{\frac{1}{2},\nu\}, \qquad (4.9)$$

we obtain $||R^{k_1}||_{V(Q_{t_1})} = 0$, which implies that for a.e. $(x,t) \in \Omega \times (0,t_1)$ we have

$$R(x,t) \leq \operatorname*{ess\,sup}_{\Omega} R_0(x).$$

The same argument is valid for the cylinders $Q_{t_s} = \Omega \times (t_{s-1}, t_s)$, $2 \leq s \leq N$, as long as their height satisfies the requirement analogue of (4.9). Thus, after a finite number of steps we obtain for the component R the estimate (4.2), for a.e. $(x,t) \in Q_T$.

In a similar way we can proceed with the other components.

5. The Discrete Maximum Principle and Stability. In this section we show that the commonly used central difference second order explicit schemes in general, violate the discrete maximum principle. Nevertheless, for these schemes, we give a theoretical proof of stability.

We work on a rectangular grid

$$x_i = i\Delta x, \quad y_j = j\Delta y, \quad t_m = m\Delta t,$$

$$i,j = 0,1,2,...M; \quad m = 0,1,2,...[T/\Delta t].$$

The spatial units are normalized such that $\Delta x = \Delta y = 1$. The approximate solution $(R^m_{ij}, G^m_{ij}, B^m_{ij})$ samples the functions:

$$R^m_{ij} \equiv U^1(i\Delta x, j\Delta y, m\Delta t),$$

$$G^m_{ij} \equiv U^2(i\Delta x, j\Delta y, m\Delta t),$$

$$B^m_{ij} \equiv U^3(i\Delta x, j\Delta y, m\Delta t).$$

On the boundary we impose the Neumann boundary condition. This corresponds to a prolongation by reflection of the image across the boundary.

We replace the second spatial derivatives and the first time derivative by a central difference and forward difference, respectively. Based on (2.4), the first element R of the color vector satisfies the following equation:

$$R_t = \frac{1}{\sqrt{g}}\mathrm{Div}(D\nabla R) \ . \qquad (5.1)$$

The diffusion matrix is written here as

$$D = \begin{pmatrix} a & b \\ b & c \end{pmatrix} ,$$

where the coefficients are given in terms of the image metric: $a = g_{22}/\sqrt{g}$; $c = g_{11}/\sqrt{g}$; $b = -g_{12}/\sqrt{g}$. With this notation, equation (5.1) is thus written as

$$R_t = \frac{1}{\sqrt{g}}((aR_x + bR_y)_x + (bR_x + cR_y)_y) \ . \tag{5.2}$$

We approximate Eq. (5.2) by the following central difference explicit scheme :

$$R_{ij}^{m+1} = R_{ij}^m + \beta \Delta t O_{ij}(R^m, G^m, B^m), \tag{5.3}$$

where $O_{ij}(R^m, G^m, B^m)$ is the discrete version of the right side of Eq. (5.1) and is given explicitly, in the central difference framework, by

$$\begin{aligned} O_{ij}= & \\ & \frac{1}{\sqrt{g}_{i,j}^m}\Big[a_{i+\frac{1}{2},j}^m(R_{i+1,j}^m - R_{i,j}^m) - a_{i-\frac{1}{2},j}^m(R_{i,j}^m - R_{i-1,j}^m) \\ & + c_{i,j+\frac{1}{2}}^m(R_{i,j+1}^m - R_{i,j}^m) - c_{i,j-\frac{1}{2}}^m(R_{i,j}^m - R_{i,j-1}^m) \\ & + \frac{1}{4}b_{i,j+1}^m(R_{i+1,j+1}^m - R_{i-1,j+1}^m) - \frac{1}{4}b_{i,j-1}^m(R_{i+1,j-1}^m - R_{i-1,j-1}^m) \\ & + \frac{1}{4}b_{i+1,j}^m(R_{i+1,j+1}^m - R_{i+1,j-1}^m) - \frac{1}{4}b_{i-1,j}^m(R_{i-1,j+1}^m - R_{i-1,j-1}^m)\Big] \ , \end{aligned} \tag{5.4}$$

where the half indices are obtained by linear interpolation. The equations for the two other color components are discretized in the same manner. This scheme is stable under CFL-like bound requirements of the time step. The stability, as well as the lack of extremum principle property, can be seen in the following theorem:

THEOREM 5.1. *If for all $m = 0, 1, 2, ..., [\frac{T}{\Delta t}]$, Δt satisfies the condition :*

$$\Delta t \leq \frac{1}{8\beta \max\limits_{i,j}\{\frac{a_{i+\frac{1}{2},j}^m}{\sqrt{g_{i,j}^m}}, \frac{a_{i-\frac{1}{2},j}^m}{\sqrt{g_{i,j}^m}}, \frac{c_{i,j+\frac{1}{2}}^m}{\sqrt{g_{i,j}^m}}, \frac{c_{i,j-\frac{1}{2}}^m}{\sqrt{g_{i,j}^m}}\}}, \tag{5.5}$$

then the solution satisfies:

$$\begin{aligned} |R_{i,j}^m| &\leq e^{S\frac{\beta}{2}t_m} \max_{i,j} |R_{i,j}^0|, \\ |G_{i,j}^m| &\leq e^{S\frac{\beta}{2}t_m} \max_{i,j} |G_{i,j}^0|, \\ |B_{i,j}^m| &\leq e^{S\frac{\beta}{2}t_m} \max_{i,j} |B_{i,j}^0|, \end{aligned} \tag{5.6}$$

where

$$S = \max_{0 \leq p \leq m} S_p, \ \textit{and,} \ S_p = \max_{i,j} \frac{|b_{i,j+1}^p|}{\sqrt{g_{ij}^p}} + \max_{i,j} \frac{|b_{i,j-1}^p|}{\sqrt{g_{ij}^p}} + \max_{i,j} \frac{|b_{i+1,j}^p|}{\sqrt{g_{ij}^p}} + \max_{i,j} \frac{|b_{i-1,j}^p|}{\sqrt{g_{ij}^p}}. \tag{5.7}$$

Proof. We give only the proof for one of the components, since for the other two, the proof is the same. We introduce the following notations:

$$L_{ij}^m = a_{i+\frac{1}{2},j}^m (R_{i+1,j}^m - R_{i,j}^m) - a_{i-\frac{1}{2},j}^m (R_{i,j}^m - R_{i-1,j}^m) \tag{5.8}$$

$$M_{ij}^m = c_{i,j+\frac{1}{2}}^m (R_{i,j+1}^m - R_{i,j}^m) - c_{i,j-\frac{1}{2},j}^m (R_{i,j}^m - R_{i,j-1}^m) \tag{5.9}$$

$$N_{ij}^m = \frac{1}{4}\Big[b_{i,j+1}^m (R_{i+1,j+1}^m - R_{i-1,j+1}^m) - b_{i,j-1}^m (R_{i+1,j-1}^m - R_{i-1,j-1}^m)\Big] \tag{5.10}$$

$$P_{ij}^m = \frac{1}{4}\Big[b_{i+1,j}^m (R_{i+1,j+1}^m - R_{i+1,j-1}^m) - b_{i-1,j}^m (R_{i-1,j+1}^m - R_{i-1,j-1}^m)\Big] \ . \tag{5.11}$$

Therefore, using (5.3) and (5.4) we can write :

$$\Big|R_{ij}^{m+1}\Big| \le \frac{1}{2}\Big|R_{ij}^m\Big| + \Big|\frac{1}{4}R_{ij}^m + \beta\frac{\Delta t}{\sqrt{g_{ij}^m}}L_{ij}^m\Big| + \Big|\frac{1}{4}R_{ij}^m + \beta\frac{\Delta t}{\sqrt{g_{ij}^m}}M_{ij}^m\Big| + \\ + \Big|\beta\frac{\Delta t}{\sqrt{g_{ij}^m}}N_{ij}^m\Big| + \Big|\beta\frac{\Delta t}{\sqrt{g_{ij}^m}}P_{ij}^m\Big| \ . \tag{5.12}$$

If $\Delta t \le \dfrac{1}{8\beta \max\limits_{i,j} \dfrac{a_{i+\frac{1}{2},j}^m}{\sqrt{g_{i,j}^m}}}$ for all $m = 0, 1, 2, ..., [\frac{T}{\Delta t}]$, then

$$\Big|\frac{1}{8}R_{ij}^m + \beta\frac{\Delta t}{\sqrt{g_{ij}^m}}a_{i+\frac{1}{2},j}^m (R_{i+1,j}^m - R_{i,j}^m)\Big| \le \max(|R_{i,j}^m|, |R_{i+1,j}^m|)\Big(\frac{1}{8} - \frac{\Delta t}{\sqrt{g_{ij}^m}}a_{i+\frac{1}{2},j}^m + \frac{\Delta t}{\sqrt{g_{ij}^m}}a_{i+\frac{1}{2},j}^m\Big) \ ,$$

which implies

$$\Big|\frac{1}{8}R_{ij}^m + \beta\frac{\Delta t}{\sqrt{g_{ij}^m}}a_{i+\frac{1}{2},j}^m (R_{i+1,j}^m - R_{i,j}^m)\Big| \le \frac{1}{8}\max_{i,j}|R_{ij}^m| \ .$$

So we can get the estimate:

$$\Big|2\cdot\frac{1}{8}R_{ij}^m + \beta\frac{\Delta t}{\sqrt{g_{ij}^m}}L_{ij}^m\Big| \le \frac{1}{4}\max_{ij}|R_{ij}^m| \quad \text{if} \quad \Delta t \le \frac{1}{8\beta \max\limits_{i,j}\{\dfrac{a_{i+\frac{1}{2},j}^m}{\sqrt{g_{i,j}^m}}, \dfrac{a_{i-\frac{1}{2},j}^m}{\sqrt{g_{i,j}^m}}\}} \ . \tag{5.13}$$

In the same way we obtain:

$$\Big|2\cdot\frac{1}{8}R_{ij}^m + \beta\frac{\Delta t}{\sqrt{g_{ij}^m}}M_{ij}^m\Big| \le \frac{1}{4}\max_{ij}|R_{ij}^m| \quad \text{if} \quad \Delta t \le \frac{1}{8\beta \max\limits_{i,j}\{\dfrac{c_{i,j+\frac{1}{2}}^m}{\sqrt{g_{i,j}^m}}, \dfrac{c_{i,j-\frac{1}{2}}^m}{\sqrt{g_{i,j}^m}}\}} \ . \tag{5.14}$$

Let

$$N_{i,j}^{m,1} = \beta\frac{\Delta t}{4\sqrt{g_{ij}^m}}b_{i,j+1}^m (R_{i+1,j+1}^m - R_{i-1,j+1}^m)$$

and

$$N_{i,j}^{m,2} = \beta\frac{\Delta t}{4\sqrt{g_{ij}^m}}b_{i,j-1}^m (R_{i+1,j-1}^m - R_{i-1,j-1}^m).$$

Then we obtain for $N_{i,j}^{m,1}$

$$|N_{i,j}^{m,1}| \leq 2 \cdot \beta \frac{\Delta t}{4\sqrt{g_{ij}^m}} |b_{i,j+1}^m| \max_{ij} |R_{i,j}^m| \ . \tag{5.15}$$

A similar inequality can be written for $|N_{i,j}^{m,2}|$, and for $|P_{i,j}^m|$. Thus we have:

$$|N_{ij}^m| \leq \beta \frac{\Delta t}{2\sqrt{g_{ij}^m}} (|b_{i,j+1}^m| + |b_{i,j-1}^m|) \max_{ij} |R_{i,j}^m| \leq \frac{\beta}{2} \Delta t (\max_{i,j} \frac{|b_{i,j+1}^m|}{\sqrt{g_{ij}^m}} + \max_{i,j} \frac{|b_{i,j-1}^m|}{\sqrt{g_{ij}^m}}) \max_{ij} |R_{i,j}^m| \,, \tag{5.16}$$

and

$$|P_{ij}^m| \leq \beta \frac{\Delta t}{2\sqrt{g_{ij}^m}} (|b_{i+1,j}^m| + |b_{i-1,j}^m|) \max_{ij} |R_{i,j}^m| \leq \frac{\beta}{2} \Delta t (\max_{i,j} \frac{|b_{i+1,j}^m|}{\sqrt{g_{ij}^m}} + \max_{i,j} \frac{|b_{i-1,j}^m|}{\sqrt{g_{ij}^m}}) \max_{ij} |R_{i,j}^m| \,. \tag{5.17}$$

¿From (5.13)–(5.17) it follows that

$$|R_{ij}^{m+1}| \leq \max_{i,j} |R_{ij}^m| \Big(1 + \frac{\beta}{2} \Delta t (\max_{i,j} \frac{|b_{i,j+1}^m|}{\sqrt{g_{ij}^m}} + \max_{i,j} \frac{|b_{i,j-1}^m|}{\sqrt{g_{ij}^m}} + \max_{i,j} \frac{|b_{i+1,j}^m|}{\sqrt{g_{ij}^m}} + \max_{i,j} \frac{|b_{i-1,j}^m|}{\sqrt{g_{ij}^m}}) \Big) \,, \tag{5.18}$$

if

$$\Delta t \leq \frac{1}{8\beta \max_{i,j} \{ \frac{a_{i+\frac{1}{2},j}^m}{\sqrt{g_{i,j}^m}}, \frac{a_{i-\frac{1}{2},j}^m}{\sqrt{g_{i,j}}}, \frac{c_{i,j+\frac{1}{2}}^m}{\sqrt{g_{i,j}^m}}, \frac{c_{i,j-\frac{1}{2}}^m}{\sqrt{g_{i,j}^m}} \}} . \tag{5.19}$$

Let

$$M_1^m = \max_{i,j} \frac{|b_{i,j+1}^m|}{\sqrt{g_{ij}^m}}, M_2^m = \max_{i,j} \frac{|b_{i,j-1}^m|}{\sqrt{g_{ij}^m}}$$

and

$$M_3^m = \max_{i,j} \frac{|b_{i+1,j}^m|}{\sqrt{g_{ij}^m}}, M_4^m = \max_{i,j} \frac{|b_{i-1,j}^m|}{\sqrt{g_{ij}^m}}.$$

Next, applying (5.18) repeatedly we find that if condition (5.19) is satisfied, then:

$$\begin{aligned} |R_{ij}^m| &\leq (1 + \frac{\beta}{2} \Delta t S_{m-1})(1 + \frac{\beta}{2} \Delta t S_{m-2}) \dots (1 + \frac{\beta}{2} \Delta t S_0) \max_{i,j} |R_{i,j}^0| \\ &\leq (1 + \frac{\beta}{2} \Delta t S)^m \max_{i,j} |R_{i,j}^0| \leq e^{\frac{\beta}{2} t_m S} \max_{i,j} |R_{i,j}^0| \ , \end{aligned}$$

where S is given in (5.7). □

The inequalities (5.6) clearly show that the maximum principle can be violated, but we still have stability. The inequalities in Theorem 5.1 show that the numerical solution is bounded in each iteration by the maximum value of the initial image multiplied by a factor. It guarantees that the flow does not blow up in finite time and ensures its stability. At the same time it is clear from the positivity of β that the maximum principle can be violated. One can actually see it in practice (see Figs. 5.1, 5.2 and 5.3). We note that this does not indicate that the scheme is not accurate. This

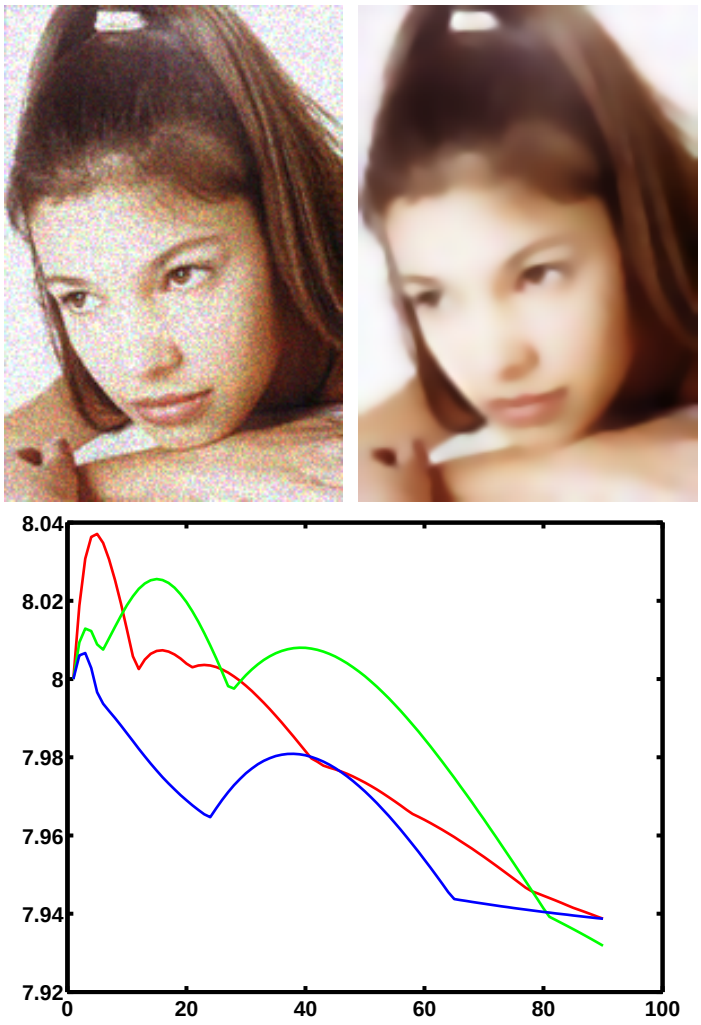

FIG. 5.1. *Top-left: Noisy Camila image. Top-right: Result of the Beltrami flow after 90 iteration. Bottom: Plot of maximum of each of the channels versus number of iterations. Parameters:* $\beta^2 = 100$, $\Delta t = 0.0091$.

situation is not unprecedented. the Crank-Nicolson scheme for the 1D heat equation, for example, is also known not to obey the maximum principle while being a useful and accurate scheme.

The reason for this discrepancy between the continuous and the discrete setting is that this second order approximation is not a non-negative one. Indeed, the mixed derivatives in (5.2) can create negative weights in certain pixels. One can easily show that a scheme which is based on a nonnegative discretization does satisfy the discrete maximum principle. Based on this result, the problem of proving the discrete maximum principle boils down to the problem of finding a nonnegative second order difference approximation. In [24], Weickert proposed a way to build a nonnegative scheme. The nonnegativity of his proposed scheme depends, however, on the condition number of the diffusion tensor D. Only in pixels where the condition number is smaller

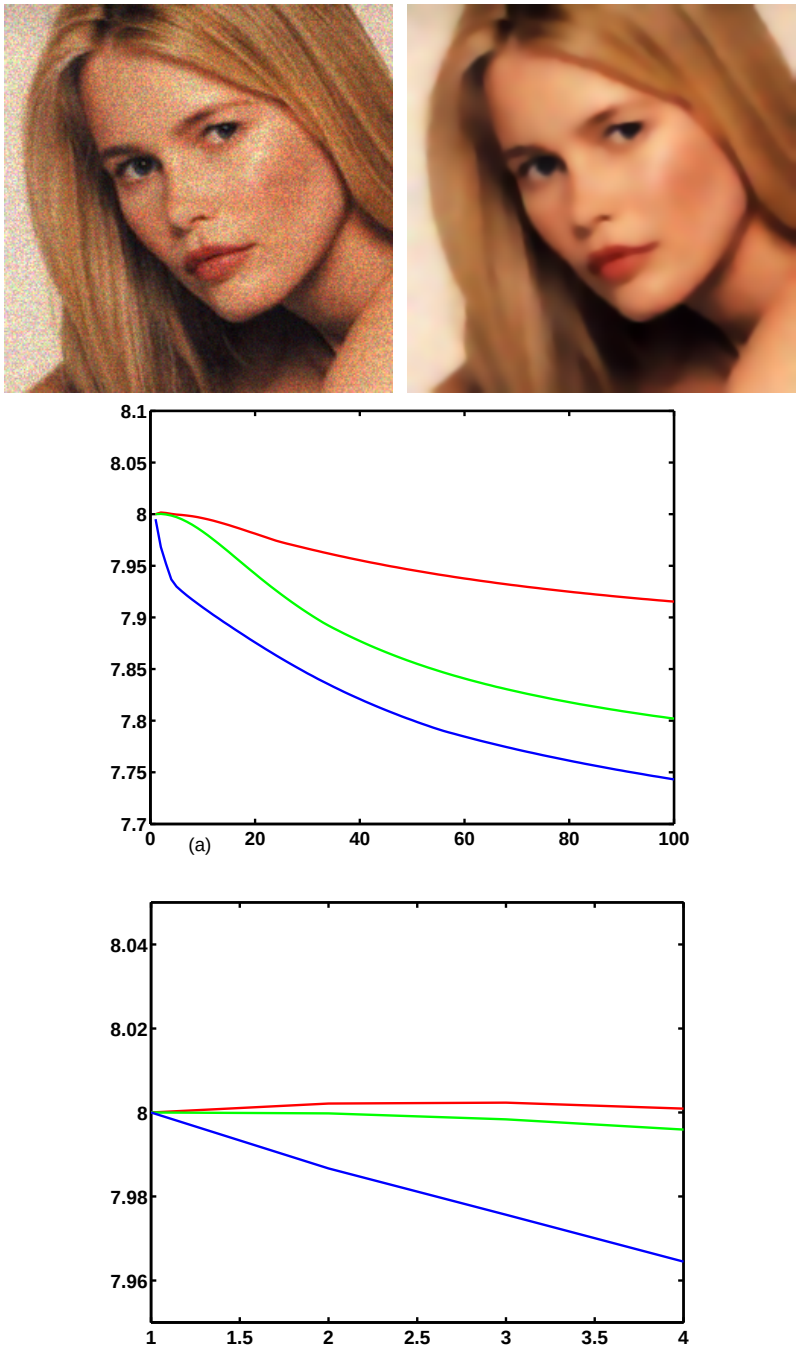

FIG. 5.2. *Top-left: Noisy Claudia image. Top-right: Result of the Beltrami flow after 100 iterations. Bottom-(a): Plot of maximum of each of the channels versus number of iterations. Bottom: Detail of the previous graph (the first 4 iterations). Parameters:* $\beta^2 = 100$, $\Delta t = 0.01$.

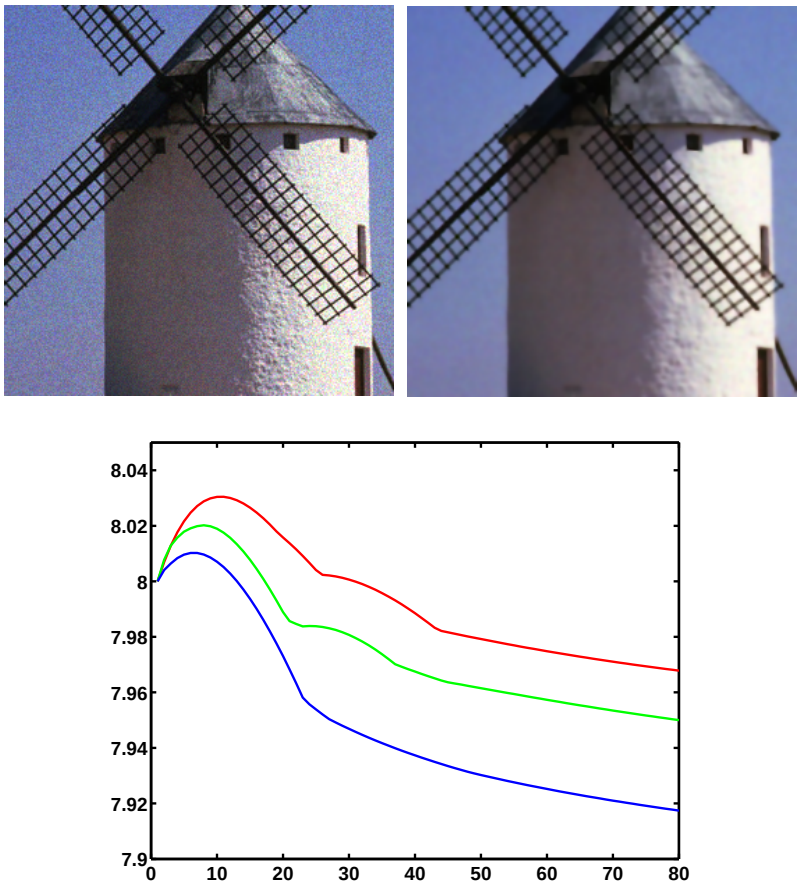

FIG. 5.3. *Top-left: Noisy windmill. Top-right: Denoised image by the Beltrami flow with after 80 iterations. Bottom: Plot of maximum of each of the channels versus number of iterations. Parameters:* β^2*=3,* $\Delta t = 0.0091$.

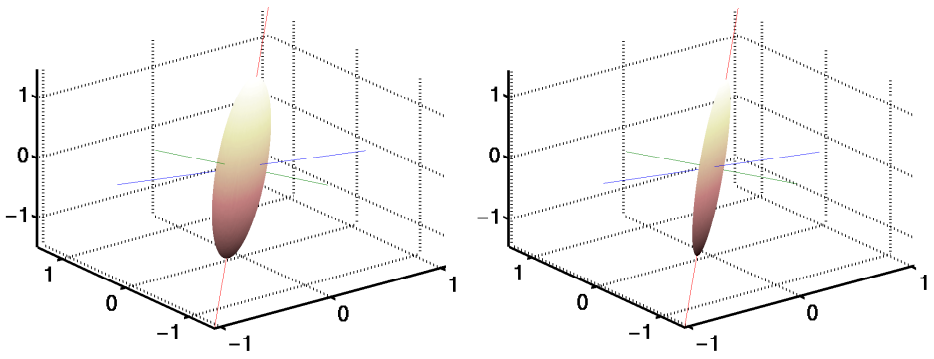

FIG. 5.4. *Camila image. Left: Ellipsoid -initial noisy data. Right: Ellipsoid- after applying Beltrami -90 iterations,* β*=10*

than $3+2\sqrt{2}$, the weights are nonnegative. This limits the application of the scheme since in many images the condition number is higher than this limit in many pixels.

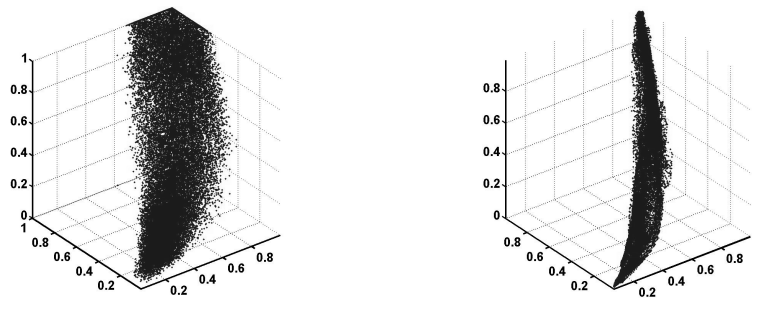

FIG. 5.5. *For Camila Image (β=10). Left: Distribution of the initial noisy data. Right: Distribution of the data after 100 iterations.*

6. Details of the Implementation and Results . In this section we present results that represent the numerical behavior of the above described numerical scheme. The initial data are given in three channels r, g and b in the range 0 to 255. We first transfer the images to the more perceptually adaptive coordinates $R = \log(1+r)$, $G = \log(1+g)$, $B = \log(1+b)$. The dynamic range of these variables is 0 to 8 and these adaptive coordinates do not limit the generality of our analysis. In the two examples presented below we corrupt the images with random noise, and denoise it using the scheme mentioned above. In the implementation, the parameters β and Δt were chosen to satisfy the stability condition (5.5).

Figures 5.1, 5.2, 5.3 all demonstrate stability of the process on one hand and the violation of the maximum principle on the other. In Figs. 5.2, 5.3, one notices that after a certain small number of iterations the maximum principle is satisfied. This is not the case in Fig. 5.1, where the violation of the maximum principle is stable and is observable over the whole evolution. The stability can also be explained by the experiments presented in Figs. 5.4 and 5.5.

Fig. 5.5 depicts the distribution of colors in the Camila image before and after the Beltrami color flow. In Fig 5.4 the ellipsoids have as principle axes the eigenvectors of the covariance-matrix of the color image. The contracting form of the ellipsoid after applying the Beltrami flow indicates a stable denoising process.

7. Concluding Remarks. In this paper, we studied the extremum principle property for the Beltrami color flow. We adapted the duality paradigm of Florack and considered "true images" as generalized functions. We therefore investigated, besides the strong solutions, also the generalized (weak) solutions. We proved the extremum principle in both the strong and the weak formulations.

We also addressed the problem of the discrete maximum principle and its close relationship with stability. In contrast to the continuous case, the discrete maximum principle cannot automatically be guaranteed. The central difference scheme does not necessarily satisfy the extremum principle. Though this property is violated, we proved the stability of the scheme. Numerical examples show, nevertheless, that this scheme is a useful tool in denoising.

Questions of existence and uniqueness as well as analysis of more elaborated numerical schemes are currently being studied .

Acknowledgements. We thank Shoshana Kamin for interesting discussions. This research has been supported in part by the Israel Academy of Science, the Tel-Aviv University fund, the Adams Super-Center for brain research, and the Israeli Ministry of Science.

REFERENCES

[1] L. Alvarez, F. Guichard, P.L. Lions, J.M. Morel," Axioms and fundamental equations of Image processing", Arch. Rational Mech. Anal. 123(1993), 199-257.

[2] V.Caselles, R.Kimmel, G.Sapiro, "Geodesic active contours", International Journal of Computer Vision,22(1997),61-79.

[3] F. Catte, P. L. Lions, J. M. Morel and T. Coll, "Image selective smoothing and edge detection by nonlinear diffusion", SIAM J. Num. Anal., vol. 29, no. 1, pp. 182-193, 1992.

[4] Y. Chen, B.C. Vemuri, Wang Li, "Image denoising and segmentation via nonlinear diffusion", Comput. Math. Appl. 39 (2000), no. 5-6, 131–149.

[5] L.Evans, "Partial differential equations", Berkeley Mathematics 1994.

[6] L. Florack, "Duality principles in Image processing and Analysis", IVCNZ 1998.

[7] D. Gilbarg, N. Trudinger, "Elliptic partial differential equations of second order", Springer-Verlag, 1977.

[8] R.A. Hummel, " Representations based on zero-crossings in scalespace ", Proc. IEEE Comp Soc. Conf. Computer Vision and Pattern Recognition, 204-209, 1986.

[9] R. Kimmel and R. Malladi and N. Sochen, "Images as Embedding Maps and Minimal Surfaces: Movies, Color, Texture, and Volumetric Medical Images", International Journal of Computer Vision 39(2) (2000) 111-129.

[10] R. Kimmel and N. Sochen, "Orientation Diffusion or How to comb a Porcupine", *Journal of Visual Communication and Image Representation* 13:238-248, 2001.

[11] R. Kimmel and N. Sochen. "Orientation Diffusion or How to Comb a Porcupine ? ", Special issue on PDEs in Image Processing, Computer Vision, and Computer Graphics, Journal of Visual Communication and Image Representation. In press.

[12] J.J. Koenderink, "The structure of images", Biol. Cybern., Vol.50, 36-370, 1984.

[13] D. Mumford, B.Gidas," Stochastic models for generic images", Quart. Appl. Math 59 (2001), no 1, 85-111.

[14] P.Perona, J.Malik,"Scale-space and edge detection using anisotropic diffusion ", IEEE Transactions on pattern Analysis and machine intelligence 12 (1990), 629-639.

[15] A. M. Polyakov, "Quantum geometry of bosonic strings", *Physics Letters*, **103B** (1981) 207-210.

[16] M. Protter and H.F. Weinberger," Maximum Principles in differential equations", Prentice-Hall,Inc., pg 65-67, 1967

[17] L. Rudin, S. Osher and E. Fatemi, " Non Linear Total Variation Based Noise Removal Algorithms", *Physica D 60 (1992), 259-268.*

[18] L. Schwartz, "Functional analysis", Courant Institute of Mathematical Sciences, 1964.

[19] N. Sochen, R. Deriche and L. Perez-Lopez, "The Beltrami Flow Over Implicit Manifolds", in Proceedings of the International Conference on Computer Vision, Nice, France 2003.

[20] N. Sochen and R. Kimmel and R. Malladi, "From high energy physics to low level vision", Report, LBNL, UC Berkeley, LBNL 39243, August, Presented in ONR workshop, UCLA, Sept. 5 1996.

[21] N. Sochen and R. Kimmel and R. Malladi, "A general framework for low level vision", *IEEE Trans. on Image Processing*, 7 (1998) 310-318.

[22] N. Sochen and Y. Y. Zeevi, "Representation of colored images by manifolds embedded in higher dimensional non-Euclidean space", Proc. IEEE ICIP'98, Chicago, 1998.

[23] N. Sochen and Y. Y. Zeevi, "Representation of images by surfaces embedded in higher

dimensional non-Euclidean space", 4th International Conference on Mathematical Methods for Curves and Surfaces, Lillehamer, Norway, July 1997.
[24] J. Weickert, " Anisotropic Diffusion in Image processing", Teubner Stuttgart, 1998.
[25] J.Weickert, "Coherence-enhancing diffusion of color images", Image and Vision Computing, Vol.17, 201-212, 1999.
[26] S. Di Zenzo , " A note on the gradient of a multiimage", Computer Vision, Graphics and Image Processing, 33:116-125, 1986.